

3D inversion of magnetotelluric phase tensor and apparent resistivity & phase data with ModEM and its application to a 250-site MT array data set from the San Andreas fault, California

Kristina Tietze¹, Oliver Ritter¹, Gary Egbert²

¹German Research Centre for Geosciences GFZ, Potsdam, Germany

²College of Earth, Ocean, and Atmospheric Sciences, Oregon State University, Corvallis, USA

SUMMARY

With advancing computational resources, three-dimensional (3D) inversion techniques have become feasible in recent years and are now a more widely used tool for magnetotelluric (MT) data interpretation. Galvanic distortion caused by small-scale near-surface inhomogeneities of dimensions remains an obstacle for 3D MT inversion which so far has experienced little attention. If not considered properly, the effect on 3D inversion can be immense and result in erroneous subsurface models and interpretations. To tackle the problem we recently implemented inversion of the distortion-free phase tensor (Caldwell et al. 2004) into the ModEM inversion package (Egbert & Kelbert 2012). We tested the new inversion using synthetic and real-world data sets. The dimensionless phase tensor components describe only variations of the conductivity structure. When inverting these data, particular care has to be taken of the conductivity structure in the a priori model, which provides the reference frame when transferring the information from phase tensors into absolute conductivity values. Our results obtained with synthetic data show that phase tensor inversion can recover the regional conductivity structure in presence of galvanic distortion if the a priori model provides a reasonable assumption for the regional resistivity average. We also used phase tensor inversion for a data set of more than 250 MT sites from the central San Andreas fault, California, where a number of sites showed significant galvanic distortion. We find the regional structure of the phase tensor inversion results compatible with previously obtained models from impedance inversion. In the vicinity of distorted sites, phase tensor inversion models exhibit more homogeneous/smooth conductivity structures.

Keywords: magnetotellurics, 3D inversion, phase tensor, galvanic distortion, static shift

INTRODUCTION

Three-dimensional interpretation of magnetotelluric (MT) by 3D inversion has become feasible and a widely used technique in recent years. Though galvanic distortion has long been recognized an obstacle for MT interpretation and been subject of research, it has only recently experienced more attention in 3D MT inversion. If 3D near-surface inhomogeneities can be integrated into the resistivity model within inversion, galvanic distortion can be modelled. However, discretization of the subsurface with sufficiently fine detail which allows for modelling of such small-scale heterogeneities (e.g. on centimetre-scale) is often impractical in 3D as the number of model parameters very rapidly exceeds manageable sizes.

Effective strategies for handling galvanically distorted MT data have been developed mainly for 2D inversion; Overviews of these methods are given in e.g. Jiracek (1990) and Jones (2011). Recently, Avdeeva et al. (2012) presented first promising results for 3D joint inversion for subsurface conductivity and galvanic distortion parameters. Alternatively, Patro et al. (2013) suggested to use phase tensor data for 3D MT inversion.

In this paper, we propose inversion of two alternative representations of the magnetotelluric impedance – the phase tensor (Caldwell et al., 2004) and apparent resistivity & phase; the first approach is similar to that of Patro et al. (2013). We implemented inversion for these two data types into the ModEM software package (Egbert & Kelbert 2012).

The phase tensor is derived from the observed impedance, but it is independent of galvanic distortion. Its invariants provide distortion-free information about the dimensionality of the underlying conductivity structure, which can be obtained directly from the observed distorted data. However, the dimensionless phase tensor components describe only variations of the conductivity structure. Thus, when inverting these data, particular care has to be taken of the conductivity structure in the a priori model, which provides the reference frame when transferring the information from phase tensors into absolute conductivity values (cf. Patro et al. 2013).

In situations, where galvanic distortion is expressed as static shift, only the amplitude of MT impedances (apparent resistivities) are affected, the phase relation is preserved. Inversion of apparent resistivity & phase data

using higher weight on the undistorted phases allows to reduce the influence of static shift on the inversion, while maintaining some of the information about the absolute subsurface conductivity contained in the apparent resistivity data. The latter has proven successful in 2D inversion (e.g. Becken et al., 2008b; Ritter et al., 2003; Tauber et al., 2003).

We tested the inversion of the new data types with synthetic and real world data sets which are affected by galvanic distortion.

METHOD

We implemented inversion for phase tensors into ModEM (Egbert & Kelbert 2012) in terms of the four real-valued phase tensor components. The approach is similar to that recently described by Patro et al. (2013).

Apparent resistivity & phase inversion uses the natural logarithm of the apparent resistivities of all four impedance components.

Therefore we appended the sensitivity calculation of ModEM software package to account for the new data types. Details on implementation are described in Tietze (2012).

SYNTHETIC DATA SET

Data set & 3D inversion setup

The synthetic data set was generated from the ObliqueConductor (OC) model displayed in Figure 1a. The main feature of the OC model is a conductive block (5 Ωm) of 30 x 10 x 9 km^3 located with its top at 2.56 km depth in the central model domain. The major axis of the block is rotated 45° from the strike direction of the regional 2D resistivity structure consisting of two half-layers of 50 Ωm and 500 Ωm . Forward responses were calculated for a 10x10-site array with 4 km site spacing (cf. Fig. 1a) using 16 frequencies between 0.001 s and 1,000 s. We also generated a randomly galvanically distorted data set by multiplying the undistorted impedances with a diagonal distortion matrix

$$\mathbf{Z}' = \mathbf{C}\mathbf{Z}, \quad \mathbf{C} = \begin{pmatrix} c_{xx} & 0 \\ 0 & c_{yy} \end{pmatrix} \quad (1)$$

simulating downward-biased static shift (Fig. 2).

3 % Gaussian noise was added to the impedance elements before calculating phase tensor and apparent resistivity & phase data from both impedance data sets.

For inversion of the synthetic data set, we used a horizontal subsurface discretization of 2 km x 2 km. We chose a starting model resistivity of 30 Ωm , which is lower than the logarithmic average of the regional resistivity (~158 Ωm). Data errors in inversion were set to 3 % of $|\mathbf{Z}_{ij}|$ for impedances, 2 % of $|\Phi_{ij}|$ for phase tensor data; for apparent resistivity we defined error floors relative to log10-decades for apparent resistivities (0.022 or 0.87 dec.) and 1° for phases.

Inversion results for undistorted data

The inversion results for undistorted data are shown in Figures 1b-d. The inversion results for impedances (Fig. 1b) and apparent resistivity & phase data (Fig. 1c) are of similarly good quality. In both results shape and location of the conductive block as well as the resistivity of the background structure are well recovered. The model derived from phase tensor data (Fig. 1d) images both the regional 2D structure as well as the conductive block. As expected, absolute resistivities and the depth location of the block are slightly underestimated as the starting model is more conductive than the true background structure.

Distorted data set

Inversion of distorted impedance or apparent resistivity and phase data revealed deep-reaching distortion of the model structures (Figs 1e-f). A very rough and incoherent pattern of resistivities can be observed in the upper layers, which can be interpreted as an attempt of the inversion to account for static shift within the model structure. The spatial extent of these artificial surface anomalies is larger than the inductive scale length and therefore alters the responses of the original 3D model. As a consequence, the image of the regional scale structure is distorted. In the example, the top of the oblique conductor and the surrounding background structure at 2.5 km depth, which is clearly resolved under normal circumstances, appears blurred. Only the very deep structure below 5 km depth is well resolved. Down-weighting apparent resistivities by increasing their errors (Fig. 1g), the OC structure can be successfully recovered by apparent resistivity & phase inversion as the phases are undistorted. In addition, the near-surface structure of these inversion models is homogeneous as in the true model.

Similar to the phase tensor inversion, resistivities and depth location of the conductive block are slightly underestimated. Phase tensor data of the distorted data set are nearly identical to those of the undistorted data set (except for the noise); hence, comparison of the result of Figure 1d to those of Figures 1e-f illustrates the value of phase tensor inversion in presence of galvanic distortion.

FIELD DATA SET

The field MT data were collected at the San Andreas fault between Parkfield and Cholame, where the fault's mechanical state changes from creeping to being locked. Between 2005 and 2008, the Geo-Electromagnetics group of GFZ Potsdam deployed more than 250 MT sites along seven parallel profiles across the fault system, covering an area of 130 km x 60 km across and along strike, respectively. 3D resistivity models derived from inversion of phase tensors and apparent resistivities & phases of the Parkfield MT data set will be presented at the workshop.

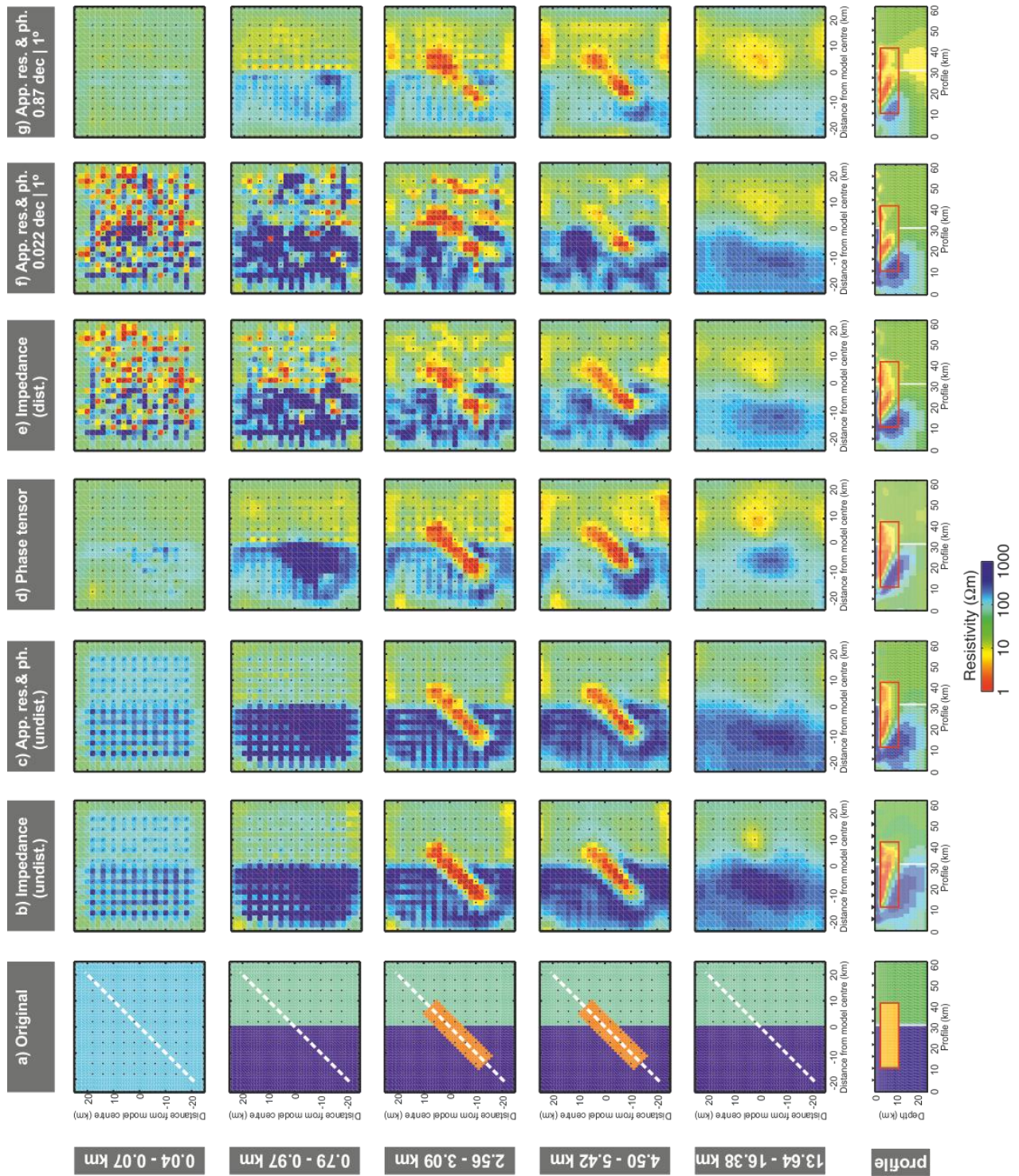


Figure 1. Synthetic model (a) and inversion results (b)-(g). (a) The main structural feature of the synthetic model is a conductive $5 \Omega\text{m}$ -block of $30 \text{ km} \times 10 \text{ km} \times 9 \text{ km}$ located with its top at 2.56 km depth in the central model domain. The major axis of the block is rotated 45° from the strike direction of the regional predominantly 2D resistivity structure consisting of two half-layers of $50 \Omega\text{m}$ and $500 \Omega\text{m}$, respectively, between 0.1 km and 75.0 km depth. The top ($< 0.1 \text{ km}$) and bottom ($> 75 \text{ km}$) layers are set to $100 \Omega\text{m}$. Black dots indicate site locations. (b)-(d): Inversion results obtained for undistorted data. (e)-(g) Inversion models for distorted data set.

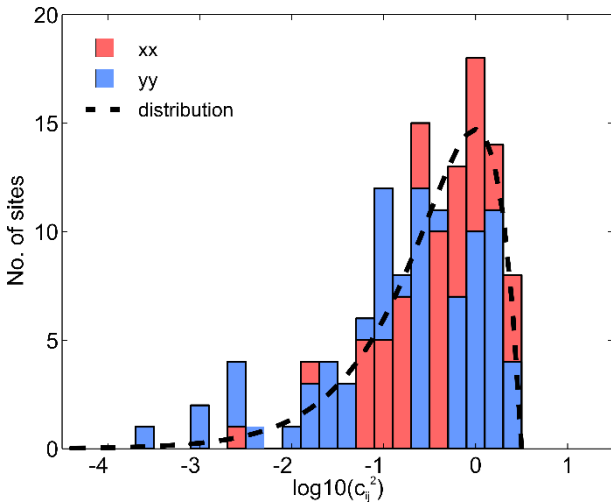


Figure 2. Statistical distribution of synthetic distortion parameters C_{xx} and C_{yy} . 100 sets distortion parameters C_{xx} and C_{yy} were estimated, so that the shift amplitudes of the apparent resistivity curves ($\log(C_{ii}^2)$) follow a modified Gamma distribution $\log(C_{ii}^2) \sim \Gamma(k; \theta) + 0.5$ with shape $k = 2.0$ and scale $\theta = 2.0$, simulating a skewed shift distribution reported for real world data sets (e.g. Sasaki & Meju, 2006). A value of $\log(C_{ii}^2) = -1$ indicates a downward shift of the corresponding apparent resistivity curve of one decade; values of 0 correspond to no shift. Distortion parameters C_{xx} and C_{yy} were randomly distributed to all 100 sites of the array.

CONCLUSION

In presence of galvanic distortion, phase tensor inversion is an efficient tool. The inversion result depends on the resistivity structure of the prior model.

Inversion of apparent resistivities & phases is applicable in 3D. If galvanic distortion is expressed as static shift, down-weighting of amplitude vs. phase is an efficient approach to reduce the influences of static shift on the inversion result also in 3D inversion.

ACKNOWLEDGMENTS

Naser Meqbel is acknowledged for helpful comments and discussions. The authors thank the Gerald W. Hohmann Memorial Trust.

REFERENCES

- Avdeeva, A., Moorkamp, M., & Avdeev, D., 2012. Three-dimensional joint inversion of magnetotelluric impedance tensor data and full distortion matrix, in *21st Workshop on Electromagnetic Induction, Darwin (Australia)*.
- Becken, M., Ritter, O., Park, S. K., Bedrosian, P. A., Weckmann, U., & Weber, M., 2008. A deep crustal fluid channel into the San Andreas Fault system near Parkfield, California, *Geophys. J. Int.*, **173**(2), 718–732.
- Caldwell, T. G., Bibby, H. M. & Brown, C., 2004. The magnetotelluric phase tensor, *Geophys. J. Int.*, **158**, 457–469.
- Egbert, G. D. & Kelbert, A., 2012. Computational Recipes for Electromagnetic Inverse Problems, *Geophys. J. Int.*, **189**(1), 251–267.
- Jiracek, G. R., 1990. Near-surface and topographic distortions in electromagnetic inductions, *Surv. Geophys.*, **11**, 163–203.
- Jones, A. G., 2011. Three-dimensional galvanic distortion of three-dimensional regional conductivity structures: Comment on Three-dimensional joint inversion for magnetotelluric resistivity and static shift distributions in complex media by Yutaka Sasaki and Max A. Meju, *J. Geophys. Res.*, **116**, B12104.
- Patro, K. P., Uyeshima, M. & Siripunvaraporn, W., 2013. Three-dimensional inversion of magnetotelluric phase tensor data, *Geophys. J. Int.*, **192**(2), 58–66.
- Ritter, O., Weckmann, U., Vietor, T., & Haak, V., 2003. A magnetotelluric study of the Damara Belt in Namibia 1. Regional scale conductivity anomalies, *Phys. Earth Planet. In.*, **138**(2), 71–90.
- Tauber, S., Banks, R., Ritter, O., & Weckmann, U., 2003. A high-resolution magnetotelluric survey of the Iapetus Suture Zone in southwest Scotland, *Geophys. J. Int.*, **153**, 548–568.
- Tietze, K., 2012. Investigating the electrical conductivity structure of the San Andreas fault system in the Parkfield-Cholame region, central California, with 3D magnetotelluric inversion, *PhD thesis*, Free University Berlin.